PNAS RESEARCH ARTICLE | NEUROSCIENCE

SPOP loss of function protects against tauopathy

Randall J. Eck[a,b], Rebecca L. Kow[b,c], Aristide H. Black[c], Nicole F. Liachko[a,b,c], and Brian C. Kraemer[a,b,c,d,e,1]

Edited by Lawrence Goldstein, Sanford Consortium for Regenerative Medicine, La Jolla, CA; received April 26, 2022; accepted November 21, 2022

The pathological accumulation of the microtubule binding protein tau drives age-related neurodegeneration in a variety of disorders, collectively called tauopathies. In the most common tauopathy, Alzheimer's disease (AD), the accumulation of pathological tau strongly correlates with cognitive decline. The underlying molecular mechanisms that drive neurodegeneration in tauopathies remain incompletely understood and no effective disease modifying pharmacological interventions currently exist. Here, we show that tau toxicity depends on the highly conserved nuclear E3 ubiquitin ligase adaptor protein SPOP in a *Caenorhabditis elegans* model of tauopathy. Loss of function mutations in the *C. elegans spop-1* gene significantly improves behavioral deficits in tau transgenic animals, while neuronal overexpression of SPOP-1 protein significantly worsens behavioral deficits. In addition, loss of *spop-1* rescues a variety of tau-related phenotypes including the accumulation of total and phosphorylated tau protein, neurodegeneration, and shortened lifespan. Knockdown of SPOP-1's E3 ubiquitin ligase *cul-3*/*Cullin3* does not improve tauopathy suggesting a non-degradative mechanism of action for SPOP-1. Suppression of disease-related phenotypes occurs independently of the nuclear speckle resident poly(A)-binding protein SUT-2/MSUT2. MSUT2 modifies tauopathy in mammalian neurons and in AD. Our work identifies SPOP as a novel modifier of tauopathy and a conceptual pathway for therapeutic intervention.

tau | neurodegeneration | Alzheimer's disease | tauopathy | *C. elegans*

Significance

We show tau toxicity depends on the highly conserved nuclear E3 ubiquitin ligase adaptor protein SPOP. Loss of *C. elegans spop-1* rescues behavioral deficits, the accumulation of tau and phosphorylated tau, neurodegeneration, and shortened lifespan in a model expressing human tau in neurons. SPOP has also been shown to be required for C9orf72 dipeptide toxicity in *C. elegans*, suggesting SPOP as a conserved regulator of protein toxicity. In contrast to dipeptide toxicity, SPOP-1 loss of function does not mimic knockdown of its ubiquitin ligase CUL-3. SPOP-1 functions in a genetic pathway parallel to SUT-2/MSUT2 to promote tau toxicity. Our work suggests SPOP as a possible therapeutic target for future intervention and provides insight into the incompletely understood mechanisms underlying tauopathy.

The pathological accumulation of the microtubule stabilizing protein tau drives age-related neurodegeneration in a variety of disorders, collectively called tauopathies. In the most common tauopathy, Alzheimer's disease (AD), the accumulation of pathological tau strongly correlates with cognitive decline (1–4). Mutations in the *MAPT* gene encoding the human tau protein directly cause familial frontotemporal dementia (FTLD) with parkinsonism-17 (5, 6). The underlying molecular mechanisms that drive disease in tauopathies remain incompletely understood, and there are no approved pharmacological interventions targeting pathological tau (7, 8).

We previously developed a model of tauopathy using the practical and genetically tractable nematode worm, *Caenorhabditis elegans. C. elegans* that expresses human tau in all neurons recapitulate phenotypes associated with tauopathy: behavioral deficits, the accumulation of insoluble and phosphorylated tau, progressive neuron death, and shortened lifespan (9). Leveraging the advantages of this model system, we have employed classical genetic mutagenesis screens, whole genome RNAi screening, and small molecule library screens to uncover new genes and pathways involved in tauopathy (10–13).

Through previous mutagenesis screens, we identified *sut-2* as a novel suppressor of tauopathy. Loss of function mutations in *sut-2*, which encodes for the nuclear poly(A)-binding protein SUT-2, reversed locomotor deficits, decreased the accumulation of insoluble tau, and reduced neurodegeneration in tau transgenic animals (12). In PS19 tauopathy mice, loss of the mammalian homolog of *sut-2*, *MSUT2*, similarly rescued learning and memory deficits, accumulation of pathological tau, and neurodegeneration. Overexpression of MSUT2 in a mouse model of tauopathy increased pathological tau deposition. In AD, MSUT2 protein levels in postmortem tissue predicted an earlier age of onset of disease, neuroinflammation, and tau pathology, demonstrating the translational utility of tau transgenic *C. elegans* in uncovering disease relevant regulators of tauopathy (14).

Here, we describe the identification and characterization of another novel suppressor of tauopathy identified by forward genetic screening: *spop-1*. SPOP (speckle-type POZ protein) is a nuclear substrate adaptor protein for the RING E3 ubiquitin ligase Cullin3 (Cul3), which selects proteins for ubiquitination in the E1-E2-E3 cascade responsible for regulated protein degradation via the proteasome (15). Genes coding for SPOP are conserved across animal phyla including mice (*SPOP*) and *C. elegans* (*spop-1*) (16, 17). SPOP localizes to nuclear speckles (NS) and contains a MATH substrate-binding domain, a BTB Cul3-binding domain, and a BACK domain which promotes oligomerization and nuclear speckle localization with BTB (Fig. 1*A*) (18, 19). There are approximately 30 known SPOP substrates which play important roles in hormone signaling and as epigenetic modifiers or signaling

Author contributions: R.J.E., R.L.K., and B.C.K. designed research; R.J.E., R.L.K., and A.H.B. performed research; R.J.E., R.L.K., and N.F.L. analyzed data; and R.J.E., R.L.K., N.F.L., and B.C.K. wrote the paper.

The authors declare no competing interest.

This article is a PNAS Direct Submission.

[1]To whom correspondence may be addressed. Email: kraemerb@uw.edu.

This article contains supporting information online at https://www.pnas.org/lookup/suppl/doi:10.1073/pnas.2207250120/-/DCSupplemental.

Published December 27, 2022.

effectors [reviewed in ref. 20]. SPOP functions as a tumor suppressor with gain of function mutations causing the development of prostate, breast, and other solid tumors (21).

In a recent publication, Snoznik et al. identified *spop-1* as essential for C9orf72 expansion-related dipeptide repeat protein (DPR) toxicity in *C. elegans*. Pathogenic repeat expansions in C9orf72 cause amyotrophic lateral sclerosis (ALS) and FTLD through a DPR-related molecular mechanism, suggesting SPOP as a conserved regulator of multiple causes of proteotoxicity (22). The *C. elegans* homolog of SPOP substrate BRD2 (bromodomain containing 2) *bet-1* was required for *spop-1* suppression of DPR toxicity, suggesting SPOP-1 acts through its function as an ubiquitin ligase adaptor protein to contribute to DPR toxicity. We found that in the case of tau, *spop-1* loss of function suppresses multiple tauopathy phenotypes but does not appear to act through the ubiquitin ligase *cul-3*. Rather, *spop-1* is required for tau toxicity in a pathway genetically parallel to *sut-2*.

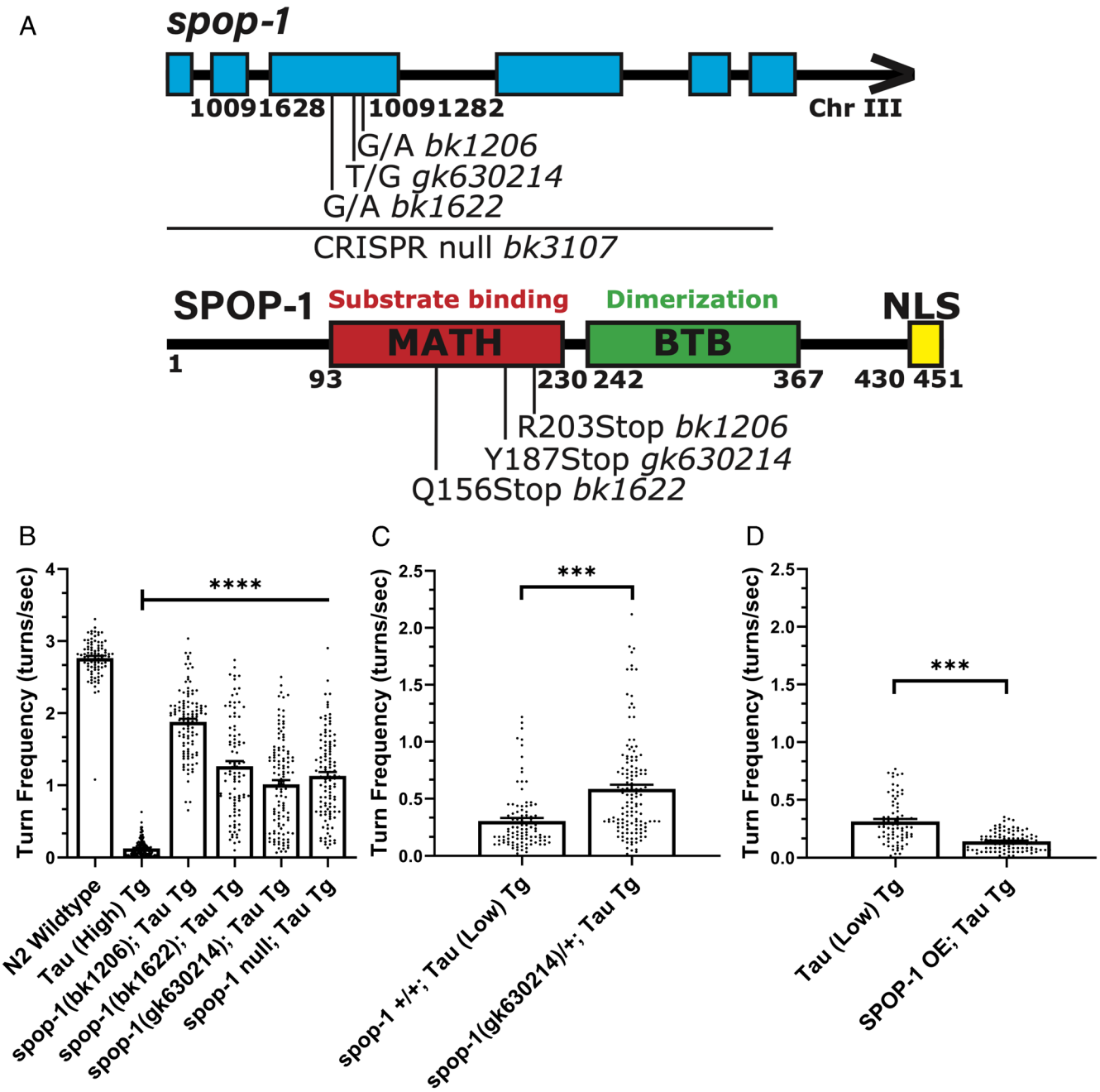

Fig. 1. SPOP-1 modifies behavioral deficits in a *C. elegans* model of tauopathy. (*A*) A diagram of *spop-1* gene (*Upper*) and SPOP-1 protein (*Lower*) with loss of function mutations used in this study. (*B*) Loss of *spop-1* rescued tau-mediated motor deficits. The tau transgenic strain CK144 expressing human 4R1N tau in all neurons was used *(bkIs144*[P*aex-3*::h4R1Ntau P*myo-2*::GFP]) (*SI Appendix*, Table S1). The mean frequency of body bends (turns/s) measured over the course of a minute and SEM are shown. Mean frequencies from left to right: 2.76, 0.13, 1.88, 1.26, 1.01, and 1.13. Statistical significance was determined by a two-way ANOVA followed by Tukey's multiple comparisons tests. N = 85 to 163. ****$P < 0.0001$ (*C*) Partial loss of *spop-1* rescued tau-mediated motor deficits. Tau Tg was CK1443 *(bkIs1443*[P*aex-3*::h4R1Ntau P*myo-2*::mCherry]). Mean frequencies from left to right: 0.30 and 0.59. Statistical significance was determined by a one-way ANOVA test. N = 99 to 132. ***$P < 0.001$. (*D*) Neuronal overexpression of SPOP-1 under the *snb-1* promotor exacerbated tau-mediated swimming motor deficits. Tau Tg was CK1443. Mean frequencies from left to right: 0.31 and 0.14. Statistical significance was determined by a one-way ANOVA test. N = 77 to 100. ***$P < 0.001$

Results

SPOP-1 Modifies Locomotor Deficits in a *C. elegans* Model of Tauopathy. We used our previously described tau transgenic *C. elegans* model to conduct a forward genetic screen for genes required for strong tauopathy-related phenotypes including uncoordinated locomotion (Unc) (9, 11, 12). We have previously demonstrated the severity of the Unc phenotype parallels neuronal dysfunction and neurodegeneration (9–12, 23–25). From this screen, we identified two strong suppressor mutations in the *sut-12* gene or the previously characterized *C. elegans bath-43*/*spop-1* gene (hereafter *spop-1*). These tau suppressing mutations introduce premature stop codons (*bk1206 – R203** and *bk1622 – Q156**) in *spop-1* (Fig. 1*A*). We obtained an additional *spop-1* loss of function allele (*gk630124 – Y187**) and generated a *spop-1* null allele (*bk3017*) by deleting the SPOP-1 coding sequence using the CRISPR/cas9 mediated genome editing system (26, 27). These *spop-1* loss of function alleles significantly rescued tau Unc phenotypes in two tau transgenic models Tau (High) Tg (Fig. 1*B*) and Tau (Low) Tg (*SI Appendix*, Fig. S1). In addition, *spop-1* loss of function did not dramatically alter locomotion in the absence of tau (*SI Appendix*, Fig. S2). The stronger suppression of behavioral phenotypes in *spop-1(bk1206)*; Tau (High) transgenic animals may be due to a linked, background mutation resulting from mutagenesis (Fig. 1*B*). Taken together, our results suggest that *spop-1* enables tau-mediated neuronal dysfunction.

To assess SPOP-1 protein levels, we generated a monoclonal antibody recognizing both human SPOP and *C. elegans* SPOP-1 proteins. Using this antibody, we detected no SPOP-1 protein in *spop-1* loss of function mutants by immunoblot (*SI Appendix*, Fig. S3). To determine whether partial loss of SPOP-1 protein suffices to rescue tau-mediated locomotor deficits, we crossed the *spop-1* allele *gk630124* into the genetic balancer hT2 (28). We found that partial loss of *spop-1* significantly improved tau-related behavioral phenotypes in Tau (Low) Tg animals but not to the level of homozygous *spop-1* loss of function, suggesting SPOP-1 protein expression levels may correspond with the severity of tau-related behavioral phenotypes (Fig. 1*C* and *SI Appendix*, Fig. S4).

To test the hypothesis that SPOP-1 protein abundance drives tauopathy phenotypes, we constructed transgenic strains that overexpress SPOP-1 protein in all neurons driven by the pan-neuronal *snb-1* promotor (23). We confirmed SPOP-1 protein overexpression in multiple, independently integrated transgenic strains by immunoblot and selected one with moderate abundance SPOP-1 protein (~ninefold increase) and one with very high abundance of SPOP-1 protein (~300-fold increase) for further functional analysis (*SI Appendix*, Fig. S5). We crossed the SPOP-1 overexpressing strain to Tau (Low) Tg animals and observed that bigenic animals exhibited significantly worsened behavioral deficits (Fig. 1*D*). We confirmed these results using another independent tau transgenic strain expressing higher levels of human tau, Tau (High) Tg animals (*SI Appendix*, Fig. S6). Moderate overexpression of SPOP-1 alone does not dramatically alter behavioral phenotypes (*SI Appendix*, Fig. S7). In addition to motility, moderate overexpression of SPOP-1 significantly increased the accumulation of tau and phosphorylated tau in Tau (High) Tg animals (*SI Appendix*, Fig. S8). Synthetic lethality analysis demonstrated that high overexpression of SPOP-1 resulted in frequent larval lethality of Tau (Low) Tg animals (*SI Appendix*, Fig. S9). Taken together, these findings support the idea that SPOP-1 protein levels drive tau-mediated neuronal dysfunction in *C. elegans*.

Mutations in *spop-1* Reduce Tau Accumulation and Rescue Neurodegeneration and Lifespan. To determine if loss of SPOP-1 improved locomotor deficits by altering tau accumulation, we next evaluated total tau levels and tau phosphorylation by immunoblot in Tau (High) Tg animals. We found that loss of function mutations in *spop-1* reduced total tau protein accumulation by more than 60% in tau transgenic animals at day 1 of adulthood (Fig. 2 *A* and *B* and *SI Appendix*, Fig. S10). We also found that the levels of tau phosphorylated at epitopes S202 and S396/S404 were decreased by over 90% (Fig. 2 *A*, *C*, and *D* and *SI Appendix*, Figs. S11 and S12) (29, 30). The dramatic reduction in total tau levels precludes our ability to fractionate for detergent insoluble tau species. However, previous evaluation of tau accumulation in human tau transgenic *C. elegans* has demonstrated that elimination of the soluble tau fraction also eliminates the insoluble tau fraction (9–14, 31). To control for SPOP-1 effects on tau transgene expression, we measured tau transgene encoded mRNA abundance by RT-PCR and found tau mRNA levels were not down-regulated (*SI Appendix*, Fig. S13). Surprisingly, mRNA levels appear to be significantly increased, a similar finding that was recently reported for tau suppressor *aly-2;aly-3* (32). This data, along with behavior and immunoblot results across multiple *spop-1* alleles and tau transgenic backgrounds, strongly suggest loss of *spop-1* does not reduce tau accumulation by transgene mRNA suppression. Our results suggest that loss of SPOP-1 significantly reduces the accumulation of pathological tau in tau transgenic animals.

During aging, tau transgenic animals experience a significant and progressive loss of their GABAergic inhibitory motor neurons, which can be visualized using an *unc-25::*GFP reporter that expresses specifically in GABAergic neurons (9). We found that loss of *spop-1* fully rescued degeneration of GABAergic motor neurons in Tau (High) Tg animals at day 1 of adulthood. This rescue was comparable to intact GABAergic motor neurons in wild-type controls, and loss of *spop-1* did not cause any apparent impact on neurons in the absence of the tau transgene (Fig. 2 *E*–*G*).

In addition to neurodegeneration, tau transgenic animals exhibit a shortened lifespan relative to non-transgenic animals (9). We found that loss of *spop-1* significantly extended the median lifespan of Tau (High) Tg animals by 2 days, comparable to the lifespan of the wild-type control (Fig. 2*H*). This result was replicated in two additional trials (*SI Appendix*, Fig. S14). While *spop-1(gk630214)* extends lifespan here, over three trials the *spop-1* loss of function alleles tested did not have any consistent lifespan extension in the absence of the tau transgene (Fig. 2*H* and *SI Appendix*, Fig. S14). Taken together, loss of SPOP-1 in tau transgenic animals reduces the accumulation of both total and phosphorylated tau protein along with a concomitant rescue of neurodegeneration and an increase in lifespan.

CUL-3 Loss of Function Does Not Recapitulate SPOP-1 Loss of Function. SPOP-1 is a putative ubiquitin ligase adaptor protein for the CUL-3 E3 ubiquitin ligase. To determine if loss of SPOP-1 suppresses tau toxicity through its function as a CUL-3 adaptor protein, we knocked down *cul-3* using RNAi in a neuronal RNAi-sensitive SID-1 overexpression background (33). If loss of SPOP-1 suppresses tau toxicity by increasing the concentration of one of its usual substrates, we would expect that knockdown of CUL-3 would also suppress tau toxicity. However, we found that knockdown of *cul-3* did not improve behavioral deficits in two independent tau transgenic strains, Tau (Low) Tg animals and Tau(V337M) Tg animals expressing mutant tau protein associated with FTLD-tau and with increased neurotoxicity (Fig. 3 *A* and *B*). We confirmed that our RNAi construct resulted in a modest *cul-3* knockdown via RT-PCR (*SI Appendix*, Fig. S15). To support these results,

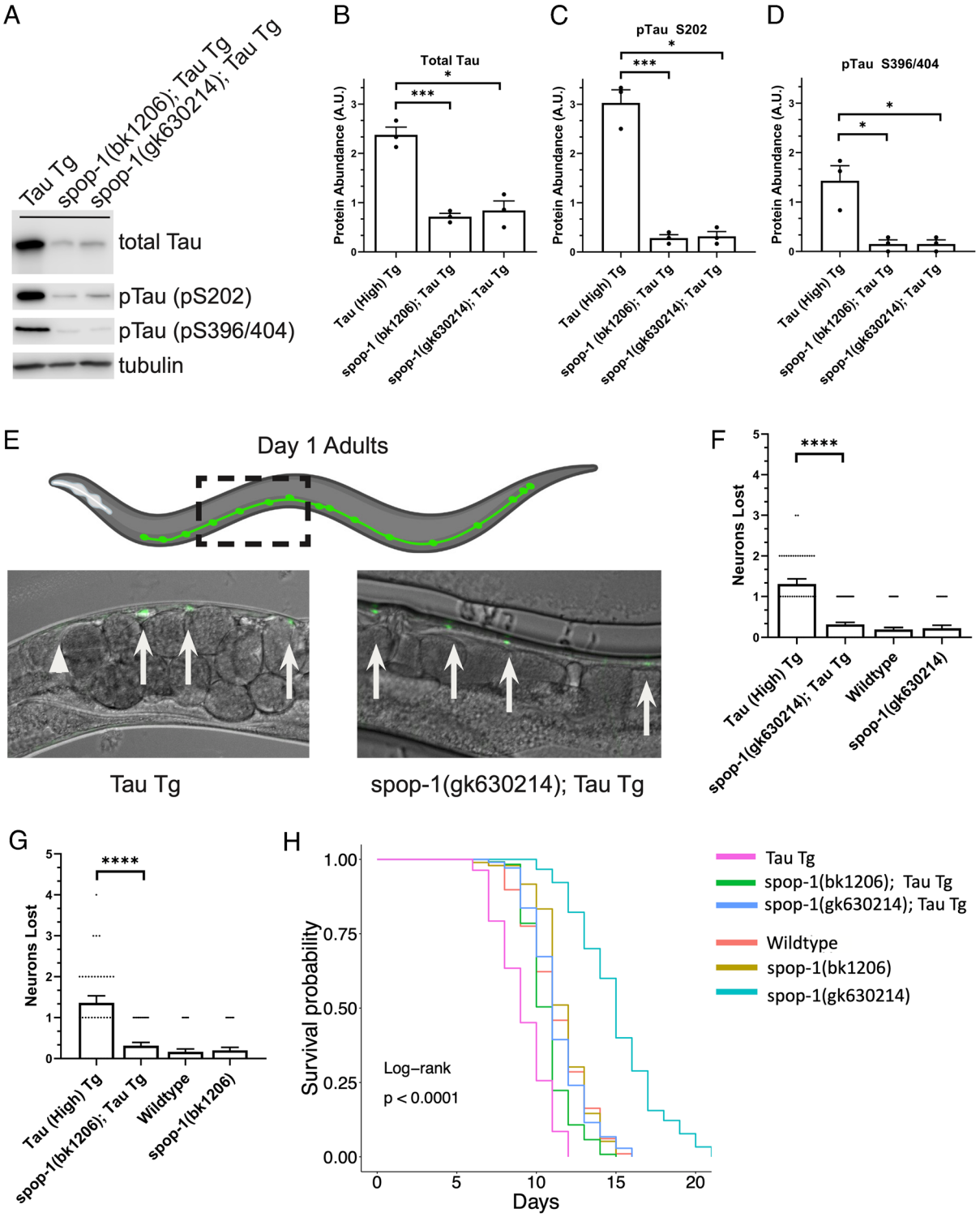

Fig. 2. Loss of *spop-1* significantly improves tau accumulation, neurodegeneration, and lifespan. (*A*) Loss of *spop-1* significantly reduced the total tau and phosphorylated tau burden in tau transgenic animals. Shown are representative immunoblots for total tau, phosphorylated tau, and tubulin of day 1 adult *C. elegans* lysates. The mouse anti-tau CP13 antibody targeting S202 and the mouse anti-tau PHF-1 antibody targeting S396 and S404 were used. Tau Tg was CK144. (*B*) Quantification of total tau. Mean and SEM are shown. Mean expression from left to right: 2.38, 0.72, and 0.84. N = 3. Statistical significance was determined by a Student's *t* test with Bonferroni correction. **P* < 0.05, ****P* < 0.001. (*C*) Quantification of pTau S202. Mean expression from left to right: 3.03, 0.28, and 0.31. N = 3, **P* < 0.05, ****P* < 0.001. (*D*) Quantification of pTau S396/S404. Mean expression from left to right: 1.43, 0.15, and 0.15. N = 3, **P* < 0.05. (*E*) Representative images showing loss of *spop-1* rescues tau-mediated neurodegeneration. GABAergic neurons marked by *punc-25::GFP* were counted in day 1 adult transgenic animals. Tau Tg was CK144. Arrowhead marks site of degenerating neuron, and arrows indicate present GABAergic neurons. (*F*) Tau transgenic animals with the *spop-1* loss of function allele *gk630214* lost an average of one less neuron per animal than tau transgenic animals. Mean neuron loss from left to right: 1.31, 0.31, 0.19, and 0.23. Statistical significance was determined by a Student's *t* test with Bonferroni correction. N = 30 to 86. *****P* < 0.0001. (*G*) Similar results were found for the *bk1206* allele. Mean neuron loss from left to right: 1.36, 0.31, 0.17, and 0.20. Statistical significance was determined by a Student's *t* test with Bonferroni correction. N = 30 to 86. *****P* < 0.0001. (*H*) Loss of *spop-1* rescued lifespan deficits in tau transgenic animals. Tau Tg was CK144. N = 82 to 121 (see *SI Appendix*, Fig. S12 for median lifespan values, pairwise comparisons, and two additional replicates).

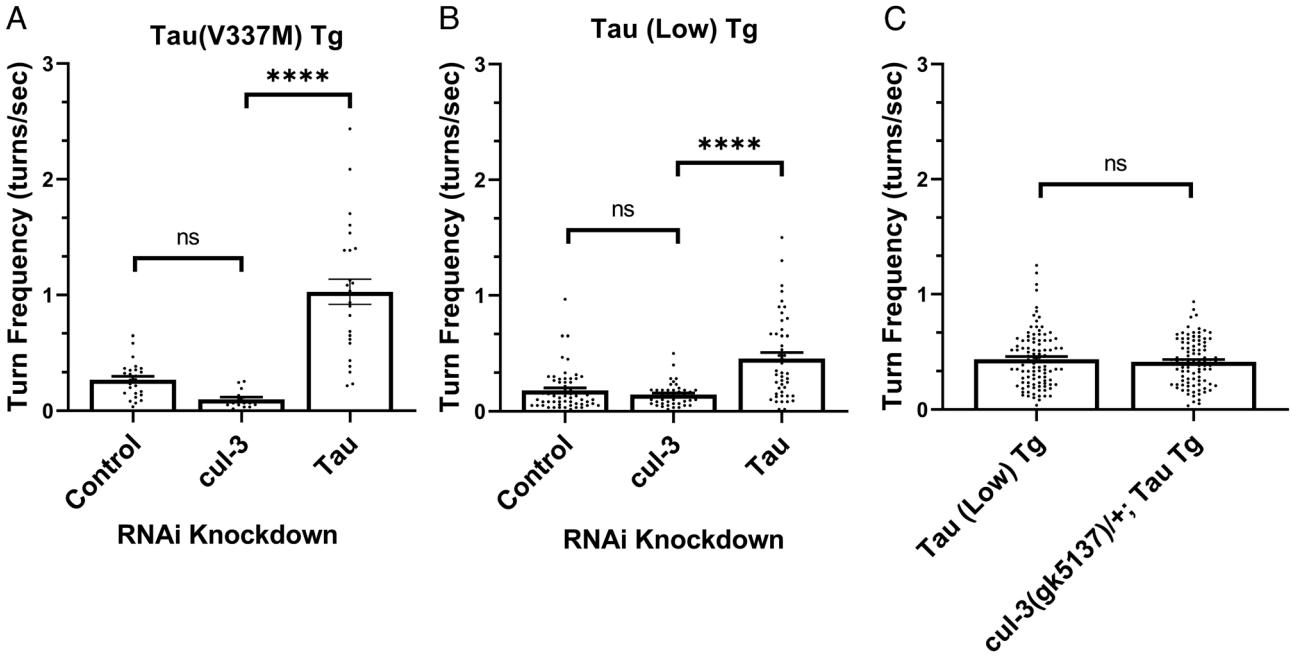

Fig. 3. Partial loss of CUL-3 does not recapitulate SPOP-1 loss of function. (*A*) RNAi knockdowns of *cul-3* did not improve locomotion in two tau transgenic strains. RNAi knockdown of tau did improve locomotion. The mean frequency of body bends (turns/s) over the course of a minute and SEM are shown. Mean frequencies from left to right: 0.27, 0.1, and 1.03. Tau Tg is CK10 (*bkIs10*[P*aes-3*::Tau V337M P*myo-2*::GFP]) (*SI Appendix*, Table S1). Statistical significance was determined by a two-way ANOVA followed by Tukey's multiple comparisons tests. N = 15 to 26, ****$P < 0.0001$. (*B*) Mean frequencies from left to right: 0.18, 0.14, and 0.46. Tau is CK1443. Statistical significance was determined by a two-way ANOVA followed by Tukey's multiple comparisons tests. N = 43 to 59, ****$P < 0.0001$. (*C*) Heterozygous loss of function of *cul-3* did not improve locomotion in one tau transgenic strain. The mean frequency of body bends (turns/s) over the course of a minute and SEM are shown. Tau Tg is CK1443. Mean frequencies from left to right: 0.44 and 0.42. Statistical significance was determined by a one-way ANOVA test. N = 95 to 101.

we obtained a *cul-3* loss of function allele, *cul-3(gk5137)*, that is homozygous lethal but heterozygous viable. Partial genetic loss of *cul-3* did not improve behavioral deficits in Tau (Low) Tg animals (Fig. 3*C*) nor did it alter locomotion on its own (*SI Appendix*, Fig. S16). In a *C. elegans* model of C9or72 dipeptide repeat toxicity, a screen of putative SPOP-1 CUL-3 substrates identified *bet-1* as necessary for muscle paralysis rescue by loss of *spop-1*. We found that a *bet-1* loss of function allele was not necessary for loss of *spop-1*'s suppression of tau motor deficits in Tau (Low) Tg animals (*SI Appendix*, Fig. S17). In addition, we undertook a targeted RNAi screen of *C. elegans* SPOP substrate homologs. No gene knockdown reproducibly reversed loss of *spop-1* suppression of tau locomotor defects in tau transgenic animals (*SI Appendix*, Fig. S18). These data suggest loss of SPOP-1 suppresses tau toxicity independent of its function as an ubiquitin ligase adaptor protein with CUL-3.

SPOP-1 Functions Independent of SUT-2 Levels in Tauopathy. To gain a mechanistic understanding of SPOP-1's role in tauopathy, we crossed the loss of function *spop-1(gk630214)* allele with a tau transgenic line overexpressing SUT-2. We have previously showed that overexpression of SUT-2, like SPOP-1, exacerbates tau behavioral deficits (23). Loss of SPOP-1 significantly rescues the uncoordinated locomotion defects caused by SUT-2 overexpression in Tau (High) Tg animals, but not to the level of *spop-1* suppression of tau in the absences of the SUT-2 transgene (Fig. 4*A*). To determine if loss of SPOP-1 rescues tau-mediated neurodegeneration by altering the level of SUT-2 protein levels, we immunoblotted for SUT-2. We found that loss of *spop-1* does not significantly alter SUT-2 protein levels in Tau (High) Tg animals (Fig. 4 *B* and *C* and *SI Appendix*, Fig. S19). To determine if the reciprocal relationship is also held, we crossed SPOP-1 overexpressing transgenic animals with tau transgenic animals with a *sut-2(bk3011)* CRISPR null allele. We found that loss of SUT-2 also rescues SPOP-1 overexpression's exacerbation of tau behavioral deficits, but not to the level of *sut-2*'s suppression of tau alone in Tau(V337M) Tg animals (Fig. 4*D*). Similarly, loss of SUT-2 did not alter SPOP-1 proteins levels in Tau(V337M) Tg animals with the CRISPR null allele *sut-2(bk3012)* (Fig. 4 *E* and *F* and *SI Appendix*, Fig. S20). Based on these experiments, *spop-1* likely acts in a parallel genetic pathway to *sut-2* in tauopathy.

Discussion

Our forward genetic screen identified two premature stop mutations in *spop-1* that rescued behavioral phenotypes in tau transgenic *C. elegans*. To confirm that *spop-1* was truly a suppressor of tauopathy in our model, we obtained an additional *spop-1* loss of function allele and generated a true *spop-1* null allele with the CRISPR cas9 genome editing system (27). All *spop-1* alleles reversed tau-mediated neurodegenerative phenotypes across multiple tau transgenic backgrounds. Overexpression of SPOP-1 in all neurons exacerbated behavioral deficits in tau transgenic animals, suggesting that SPOP-1 protein levels play a role in tauopathy.

We found that SPOP-1's role in tauopathy was not mediated by its UPS substrate bromodomain protein BET-1, the ortholog of human BRD2, as has been shown to be the case in DPR toxicity (22). In fact, knockdown of *cul-3*, the ortholog of human *Cul3*, and a set of known targets of SPOP conserved in *C. elegans* revealed SPOP-1's known or conserved functions as a nuclear ubiquitin ligase adaptor for CUL-3 degradation substrates is likely not responsible for its critical role in tauopathy, though further study is required. However, we did find that *spop-1* and *sut-2* function in parallel genetic pathways in tauopathy. We recently showed that SUT-2 acts epistatically to two poly(A) nucleases *ccr-4* and *parn-2*, suggesting control of poly(A) RNA metabolism plays a role in SUT-2 function in tauopathy (27). The mechanism of SPOP-1 action in tauopathy remains to be further explored.

In our previous genetic studies of tauopathy in *C. elegans*, we uncovered several genes whose loss of function suppresses tau-mediated

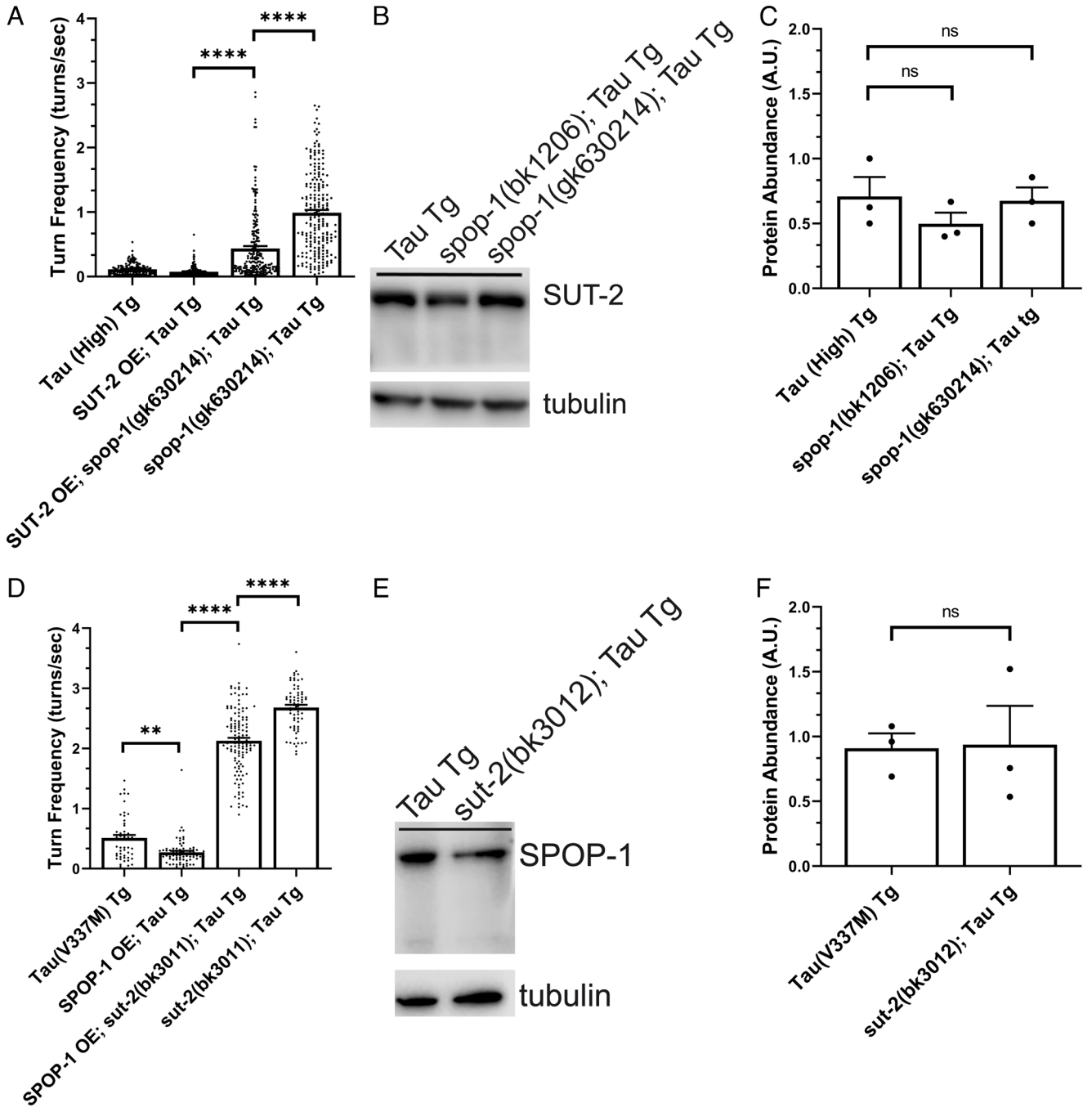

Fig. 4. SPOP-1 acts independent of SUT-2 levels in tauopathy. (*A*) Loss of *spop*-1 partially rescued the exacerbation of tau locomotor deficits by the overexpression of SUT-2 in tau transgenic animals. Tau Tg was CK144. Mean frequency of body bends (turns/s) and SEM are shown. Mean frequencies from left to right: 0.11, 0.08, 0.44, and 0.99. Statistical significance was determined by a two-way ANOVA followed by Tukey's multiple comparisons tests. N = 161 to 220. ****P < 0.0001. (*B*) Loss of *spop-1* did not significantly affect SUT-2 protein levels. Shown are representative immunoblots images (12). (*C*) Quantification of SUT-2 protein levels. Mean expression from left to right: 0.71, 0.45, and 0.67. N = 3 (*D*) Loss of *sut-2(bk3011)* partially rescued the exacerbation of tau locomotor deficits by the overexpression of SPOP-1 in tau transgenic animals. Tau Tg was CK10 (bkIs10[Paes-3::Tau V337M Pmyo-2::GFP]) (*SI Appendix*, Table S1). Mean frequencies from left to right: 0.51, 0.27, 2.13, and 2.68. N = 52 to 128. **P < 0.01, ****P < 0.0001. (*E*) Loss of *sut-2(bk3012)* did not significantly affect SPOP-1 protein levels. Shown are representative immunoblots images. (*F*) Quantification of SPOP-1 protein levels. Mean expression from left to right: 0.91 and 0.94. N = 3.

phenotypes and neurodegeneration (suppressor of tauopathy or *sut* genes) (11, 12, 27). The largest group of *sut* genes isolated to date, including *spop-1*, encode proteins residing in NS (*sut-1, sut-2*, *aly-1*, *aly-2*, *aly-3*, *parn-2*, *spop-1*) (11, 12, 27, 32). Taken together, these modifiers suggest a possible mechanistic pathway involving NS in tauopathy. NS are phase-separated nuclear assemblies that store and modify factors involved in the processing of mRNA (34). The first tauopathy suppressor isolated, *sut-1*, encodes a protein that localizes to NS and is thought to mediate trans-spliceosome recycling (11, 35). The SUT-2 protein and its human homolog MSUT2 reside in NS and bind to poly(A) RNA (14, 23). The three *C. elegans* homologs of mRNA nuclear export complex component ALYREF, *aly-1, aly-2, and aly-3,* code for proteins in NS in addition to suppressing tauopathy (32). The *parn-2* gene encodes a protein known to reside in NS and also has poly(A) RNAse activity. Finally, SPOP localizes to NS undergoing liquid–liquid phase separation mediated by interactions between its BTB and BACK domains and substrates (19, 27).

The disruption of NS and the core NS scaffold protein SRRM2 have been directly implicated in neurodegenerative disease (36–39). Tanaka and colleagues found the nuclear depletion of phosphorylated SRRM2, a core NS scaffold protein, destabilized PQBP1 impairing synapses in an in vitro and mouse model of amyloid beta aggregation, characteristic of AD (37). Lester and colleagues found that tau sequesters SRRM2 into RNA-rich cytoplasmic aggregates in vitro, disrupting NS in model systems (36). We found SRRM2 is depleted from the nucleus of AD patient neurons compared to age-matched controls and colocalizes with cytoplasmic tau aggregates. Additionally, SRRM2 cytoplasmic accumulation in the frontal cortex correlated with age of onset of disease (38). Independent of its function with Cul3, the loss of SPOP may change the composition of NS, possibly modifying tau-mediated disruption of NS or tau toxicity. LLPS has also been implicated widely in neurodegenerative disease (40). The loss of SPOP BTB and BACK domains may also change the phase separation landscape of NS. Alternatively, SPOP may directly interact with tau in the nucleus in tauopathy or mislocalize to the cytoplasm and interact with novel UPS substrates. Previous immunofluorescent experiments in *C. elegans* models of tauopathy have not detected any obvious nuclear tau, limiting the exploration of this question, but the existence of low abundance nuclear tau species cannot be excluded as a possibility by these experiments (9, 12, 25). Future experiments should identify whether SPOP phase separation participates in disease mechanisms of tauopathy and, once the SPOP mediated mechanism of tauopathy is understood, exploit this novel neuroprotective pathway therapeutically.

Materials and Methods

***C. elegans* Strains, Genome Editing, Mutagenesis, and Transgenic Animals.** The wild-type *C. elegans* control strain used was N2 (Bristol) (*SI Appendix*, Table S1) (41). The *C. elegans* alleles used in this study *bk1206* and *bk1622* were generated through chemical mutagenesis as previously described and subsequently outcrossed 3× (11, 42). The *spop-1* null allele *bk3107* was generated using the CRISPR Cas9 genome editing technology using ALT-R reagents (Integrated DNA Technologies) including recombinant Cas9 protein and synthetic CRISPR guide RNAs as described (27, 43, 44). The following crRNA guide sequences (GAUAUCUAUGAUAUGACAG and CUAUGAUUGAUGCCCUCACA) targeting the 3′ and 5′ ends of the *spop-1* coding region were used. All other strains were obtained from the *C. elegans* Genetics Center. *C. elegans* mutants were crossed into tau transgenic lines CK144 (*bkIs144*[P*aex-3*::h4R1Ntau P*myo-2*::GFP]) and CK1443 transgenic animals *(bkIs1443*[P*aex-3*::h4R1Ntau P*myo-2*::mCherry]) expressing human 4R1N tau as well as CK10 (*bkIs10*[Paex-3::Tau V337M P*myo-2*::GFP]) expressing mutant human tau (11, 31). All strains were maintained at 20 °C on NGM plates seeded with OP50 *Escherichia coli* (41). Genotypes were confirmed by PCR and sequencing or restriction digests for all strains with non-obvious phenotypes.

Behavior in *C. elegans*. NGM plates of day 1 adult *C. elegans* were flooded with 1 mL of M9 buffer, and swimming worms were pipetted onto a 35 mm unseeded NGM plate. Approximately 30 s following the addition of M9 buffer, worms were recorded swimming for 1 min at 14 frames per second. These videos were captured and analyzed with WormLab 2019 (MBF Bioscience). The frequency of body bends, or turns, as defined as a change in body angle of a least 20° from a straight line measured by the quarter points and midpoint of the worms, was quantified as a readout of locomotion. Worms tracked for less than 40 s were omitted from this analysis. At least three independent samples totaling approximately 80 worms per strain were counted for every comparison (27).

SPOP Antibody Preparation. Human SPOP is highly homologous to *C. elegans* SPOP-1 with 65.9% amino acid homology. We raised monoclonal antibodies against human SPOP by producing recombinant SPOP as a 6×His tagged protein in *E. coli* and used the purified full length SPOP protein as an immunogen to inject naïve BALB/C mice. All mAb production work was conducted at the Washington State University Monoclonal Antibody Center as a fee for service project. Human SPOP reactive mAb clones were screened for reactivity against *C. elegans* SPOP-1 protein, and clone 8B was selected for its specificity (*SI Appendix*, Fig. S3).

Assessment of Synthetic Lethality. Tau transgenic animals overexpressing SPOP-1 in all neurons were crossed with wild-type male worms to create F1 populations heterozygous for both the tau transgene, marked by GFP fluorescence in the pharynx, and SPOP-1 neuronal overexpression, marked by mCherry fluorescence in the body wall. From a single F1 parent, each F2 progeny was scored for homozygous, heterozygous, or no transgene expression for both tau and SPOP-1 overexpression. Animals that did not survive past L2 were omitted. A chi-squared analysis was performed to assess significance (24).

Lifespan Assay. *C. elegans* was grown on NGM plates at 20 °C from a timed egg lay coordinated to synchronize all strains at L4 stage. L4 worms were transferred onto 35 mm NGM plates seeded with 10× concentrated OP50 and treated with 10 mg/mL 5-fluorodeoxyuridine to prevent reproduction. Each plate was blinded. Approximately, 100 worms per strain were assayed at 25 °C daily for signs of locomotion and pharyngeal pumping. Worms lacking signs of movement were tapped lightly with a platinum pick to provoke a response. Worms lacking signs of movement were counted as dead and removed from the plate. Worms which died of bursting or mishandling were omitted from analysis. Chi-squared analysis with a Mantel–Cox test was used to determine statistical significance in R (24).

GABAergic Neuron Loss Assay. GABAergic inhibitory motor neurons were visualized by the expression of GFP under the *unc-25* promoter (P*unc*-25::GFP). This reporter strain (CZ1200) was crossed into tau transgenic animals to assay neurodegeneration by GABAergic neuron loss. Day 1 adult worms were immobilized on a 2% agarose pad with 0.01% sodium azide. A subset of VD and DD GABAergic neurons were assayed live with fluorescent microscopy using an Olympus 40× dry objective and a 60× oil objective on the DeltaVision Elite (Applied Precision) system. The number of live neurons was scored. A Student's *t* test with Bonferroni correction was used to determine statistical significance in R (12).

***C. elegans* RNA Extraction and Quantitative PCR.** RNA was purified from day 1 adult snap-frozen *C. elegans* pellets using TRIzol Reagent (Thermo Fisher Scientific, Inc.) per manufacturer's protocol. A NanoPhotometer® NP80 spectrophotometer (Implen GmbH) was used to access RNA concentration and quality following resuspension in 50 µL sterile water. Any DNA contamination was then removed from the RNA sample using the DNA-free™ Kit (Thermo Fisher) per manufacturer's protocol. cDNA and NoRT negative controls were synthesized using iScript™ Reverse Transcription Supermix for RT-qPCR (Bio-Rad Laboratories, Inc.) per manufacturer's protocol. We performed quantitative PCR using the iTaq™ Universal SYBR® Green Supermix kit (Bio-Rad), a 96 well plate, and the CFX Connect Real-Time PCR Detection System (Bio-Rad). The primer set for the human MAPT gene was forward primer: 5′-GTGTGGCTCATTAGGCAACATCC-3′ and reverse primer: 5′-CGTTCTCGCGGAAGGTCAG-3. The primer set for *C. elegans rpl-32* was forward primer: 5′-GGTCGTCAAGAAGAAGCTCACCAA-3′ and reverse primer: 5′-TCTGCGGACACGGTTATCAATTCC-3′. The primer set for *C. elegans cul-3* was forward primer: 5′-GCTCCGGTAATGGTGGACAACAAA-3′ and reverse primer: 5′ -GCGGTAGAGCTCCTCGAAACTCAAG-3′. The primer set for *C. elegans act-1* was forward primer: 5′-AGCCATCCTTCTTGGGTATG-3′ and reverse primer: 5′-ATTCCTGGGTACATGGTGGT-3′. Each genotype was tested in three to five biological replicates and three technical replicates. MAPT or *cul-3* mRNA levels were normalized to *rpl-32 or act-1*, internal reference control genes, following the delta-delta CT method (24).

Tau Extraction and Immunoblotting. *C. elegans* was grown from hypochlorite-purified eggs at 20 °C for 3 days on 5XPEP plates until young adults. Worms were washed off plates with M9 buffer, collected by centrifugation, and snap-frozen in liquid nitrogen to be stored at −70 °C. These protein samples were thawed and then diluted with 2 × SDS protein sample buffer (0.046 M Tris, 0.005 M EDTA, 0.2 M dithiothreitol, 50% sucrose, 5% sodium dodecyl sulfate, 0.05% bromophenol blue), adding four times the volume (µL) of buffer to the weight of the pellet (mg). Samples were sonicated at 70% for 15 s three times returning to ice between each replicate, boiled for 10 min at 95 °C, centrifuged at 13,000 × g for 2 min, and stored at −20 °C. Samples were loaded (10 µL) onto 4 to 15% precast criterion sodium dodecyl sulfate polyacrylamide gel electrophoresis gradient gels and transferred to PVDF per manufacturer's protocol (Bio-Rad). The ladder is Precision Plus Protein Standards (Bio-Rad). The primary antibodies used were rabbit monoclonal anti-tau SP70

antibody (Rockland) at 1:5,000, mouse anti-tubulin antibody E7 (Developmental Studies Hybridoma Bank) at 1:5,000, mouse anti-tau CP13 antibody (Peter Davies) at 1:1,000, mouse anti-tau PHF-1 antibody (Peter Davies) at 1:1,000, and mouse anti-SPOP antibody at 1:250 or 1:100. The secondary antibodies used were anti-rabbit HRP (Jackson Immuno Research) and anti-mouse HRP (Jackson Immuno Research) at 1:5,000 (29, 30). ECL substrate was used to visualize the membrane (Bio-Rad). Chemiluminescence signals were detected with the ChemiDoc-It Imager (Analytik Jena US, Inc.) and quantified with Fiji (45). A Student's *t* test with Bonferroni correction was used to determine statistical significance in R.

RNAi Treatment. SID-1 was overexpressed in all neurons in tau transgenic animals by crossing into the neuronal RNAi enhancer TU3311 to increase the efficiency of RNAi treatment (33). *E. coli* clones (HT115) from the *C. elegans* genome RNAi library (from the United Kingdom Molecular Research Council Recourse Center), and the *C. elegans* ORFeome cloning project (46) was grown on NGM media with 25 μg/mL carbenicillin and 1 mM isopropyl-β-D-thiolgalactopyranoside to induce double-stranded RNA expression (42). Hypochlorite-purified eggs were seeded onto the bacterial lawns of these plates, and day 1 adult worms were scored on the plate and for swimming locomotor deficits as described above for enhancement or suppression of *spop-1* loss of function's suppression of tauopathy (10). The same protocol was followed for RT-PCR analysis except eggs were seeded onto 150 mm, instead of 60 mm, plates. Screening of RNAi clones was blinded. Included controls were empty vector L4440, *unc-22* (positive control, worsened phenotype), and tau (positive control, improved phenotype).

Statistical Analysis. Statistical significance was determined using R: A language and environment for statistical computing (R Foundation for Statistical Computing, Vienna, Austria). Statistical significance is demarcated in figures as $*P < 0.05$, $**P < 0.01$, $***P < 0.001$, and $****P < 0.0001$. Graphing was performed using the Prism V8.4.3 software package (GraphPad by Dotmatics, Bishop's Stortford, United Kingdom).

Data, Materials, and Software Availability. All study data are included in the article and/or *SI Appendix*.

ACKNOWLEDGMENTS. We thank Victoria Hulubei at WSU mAb Center for outstanding technical assistance in producing SPOP-1 reactive mAbs. We thank Aleen Saxton, Brandon Henderson, Jade Stair, and Isaac Miller for outstanding technical assistance in media preparation. We thank Aleen Saxton for sharing her technical expertise in *C. elegans* husbandry. This work was supported by grants from the National Institute of Health [R01 NS064131 (B.C.K), R01AG066729 (N.F.L.), and CMB Training Grant T32 GM007270 (R.J.E.)] and the United States (U.S.) Department of Veterans Affairs (VA) Biomedical Laboratory Research and Development Service [Merit Review Grant #I01BX004044 (N.F.L.), Merit Review Grant #I01BX005742 (B.C.K.)]. Some strains were provided by the Caenorhabditis Genetics Center, which is funded by National Institute of Health's Office of Research Infrastructure Programs (P40 OD010440), and by the Reverse Genetics Core Facility at the University of British Columbia, which is part of the international *C. elegans* Gene Knockout Consortium. We thank WormBase for essential *C. elegans* model organism information. We thank Peter Davies and Virginia Lee for anti-tau antibodies. We thank Dionne Vafeados and Robert Waterston for providing RNAi clones from the *C. elegans* ORFeome project. Some figures were made in Adobe InDesign and BioRender.

Author affiliations: [a]Graduate Program in Neuroscience, University of Washington, Seattle, WA 98195; [b]Division of Gerontology and Geriatric Medicine, Department of Medicine, University of Washington, Seattle, WA 98104; [c]Geriatrics Research Education and Clinical Center, Veterans Affairs Puget Sound Health Care System, Seattle, WA 98108; [d]Department of Psychiatry and Behavioral Sciences, University of Washington, Seattle, Washington 98195; and [e]Department of Laboratory Medicine and Pathology, University of Washington, Seattle, Washington 98195

1. L. M. Bierer *et al.*, Neocortical neurofibrillary tangles correlate with dementia severity in Alzheimer's disease. *Arch. Neurol.* **52**, 81–88 (1995).
2. K. P. Riley, D. A. Snowdon, W. R. Markesbery, Alzheimer's neurofibrillary pathology and the spectrum of cognitive function: Findings from the Nun Study. *Ann. Neurol.* **51**, 567–577 (2002).
3. P. Tiraboschi *et al.*, Alzheimer disease without neocortical neurofibrillary tangles: "A second look". *Neurology* **62**, 1141–1147 (2004).
4. P. T. Nelson *et al.*, Correlation of Alzheimer disease neuropathologic changes with cognitive status: A review of the literature. *J. Neuropathol. Exp. Neurol.* **71**, 362–381 (2012).
5. D. J. Irwin, Tauopathies as clinicopathological entities. *Parkinsonism Relat. Disord.* **22**, S29–33 (2016).
6. Y. Wang, E. Mandelkow, Tau in physiology and pathology. *Nat. Rev. Neurosci.* **17**, 5–21 (2016).
7. J. Götz, G. Halliday, R. M. Nisbet, Molecular pathogenesis of the tauopathies. *Annu. Rev. Pathol.* **14**, 239–261 (2019).
8. S. Jadhav *et al.*, A walk through tau therapeutic strategies. *Acta. Neuropathol. Commun.* **7**, 22 (2019).
9. B. C. Kraemer *et al.*, Neurodegeneration and defective neurotransmission in a Caenorhabditis elegans model of tauopathy. *Proc. Natl. Acad. Sci. U.S.A.* **100**, 9980–9985 (2003).
10. B. C. Kraemer, J. K. Burgess, J. H. Chen, J. H. Thomas, G. D. Schellenberg, Molecular pathways that influence human tau-induced pathology in Caenorhabditis elegans. *Hum. Mol. Genet.* **15**, 1483–1496 (2006).
11. B. C. Kraemer, G. D. Schellenberg, SUT-1 enables tau-induced neurotoxicity in C. elegans. *Hum Mol. Genet.* **16**, 1959–1971 (2007).
12. C. R. Guthrie, G. D. Schellenberg, B. C. Kraemer, SUT-2 potentiates tau-induced neurotoxicity in Caenorhabditis elegans. *Hum. Mol. Genet.* **18**, 1825–1838 (2009).
13. A. V. McCormick, J. M. Wheeler, C. R. Guthrie, N. F. Liachko, B. C. Kraemer, Dopamine D2 receptor antagonism suppresses tau aggregation and neurotoxicity. *Biol. Psychiatry* **73**, 464–471 (2013).
14. J. M. Wheeler *et al.*, Activity of the poly(A) binding protein MSUT2 determines susceptibility to pathological tau in the mammalian brain. *Sci. Transl. Med.* **11**, eaao6545 (2019).
15. J. E. Kwon *et al.*, BTB domain–containing speckle-type POZ protein (SPOP) serves as an adaptor of Daxx for ubiquitination by Cul3-based ubiquitin ligase. *J. Biol. Chem.* **281**, 12664–12672 (2006).
16. Y. Nagai *et al.*, Identification of a novel nuclear speckle-type protein, SPOP. *FEBS Lett.* **418**, 23–26 (1997).
17. C. J. Huang, H. Y. Chen, W. Y. Lin, K. B. Choo, Differential expression of speckled POZ protein, SPOP: Putative regulation by miR-145. *J. Biosci.* **39**, 401–413 (2014).
18. M. Zhuang *et al.*, Structures of SPOP-substrate complexes: Insights into molecular architectures of BTB-Cul3 ubiquitin ligases. *Mol. Cell.* **36**, 39–50 (2009).
19. M. R. Marzahn *et al.*, Higher-order oligomerization promotes localization of SPOP to liquid nuclear speckles. *EMBO J.* **35**, 1254–1275 (2016).
20. M. J. Cuneo, T. Mittag, The ubiquitin ligase adaptor SPOP in cancer. *FEBS J.* **286**, 3946–3958 (2019).
21. R. S. Mani, The emerging role of speckle-type POZ protein (SPOP) in cancer development. *Drug. Discov. Today* **19**, 1498–1502 (2014).
22. C. Snoznik *et al.*, The nuclear ubiquitin ligase adaptor SPOP is a conserved regulator of C9orf72 dipeptide toxicity. *Proc. Natl. Acad. Sci. U.S.A.* **118** (2021).
23. C. R. Guthrie, L. Greenup, J. B. Leverenz, B. C. Kraemer, MSUT2 is a determinant of susceptibility to tau neurotoxicity. *Hum. Mol. Genet.* **20**, 1989–1999 (2011).
24. L. M. Taylor *et al.*, Pathological phosphorylation of tau and TDP-43 by TTBK1 and TTBK2 drives neurodegeneration. *Mol. Neurodegener.* **13**, 7 (2018).
25. S. M. Waldherr, T. J. Strovas, T. A. Vadset, N. F. Liachko, B. C. Kraemer, Constitutive XBP-1s-mediated activation of the endoplasmic reticulum unfolded protein response protects against pathological tau. *Nat. Commun.* **10**, 4443 (2019).
26. O. Thompson *et al.*, The million mutation project: A new approach to genetics in Caenorhabditis elegans. *Genome Res* **23**, 1749–1762 (2013).
27. R. L. Kow *et al.*, Distinct Poly(A) nucleases have differential impact on sut-2 dependent tauopathy phenotypes. *Neurobiol. Dis.* **147**, 105148 (2021).
28. K. S. McKim, T. Starr, A. M. Rose, Genetic and molecular analysis of the dpy-14 region in Caenorhabditis elegans. *Mol. Gen. Genet.* **233**, 241–251 (1992).
29. L. Otvos *et al.*, Monoclonal antibody PHF-1 recognizes tau protein phosphorylated at serine residues 396 and 404. *J. Neurosci. Res.* **39**, 669–673 (1994).
30. K. Duff *et al.*, Characterization of pathology in transgenic mice over-expressing human genomic and cDNA tau transgenes. *Neurobiol. Dis.* **7**, 87–98 (2000).
31. S. J. Benbow, T. J. Strovas, M. Darvas, A. Saxton, B. C. Kraemer, Synergistic toxicity between tau and amyloid drives neuronal dysfunction and neurodegeneration in transgenic C. elegans. *Hum Mol. Genet.* **29**, 495–505 (2020).
32. R. L. Kow, A. H. Black, A. D. Saxton, N. F. Liachko, B. C. Kraemer, Loss of aly/ALYREF suppresses toxicity in both tau and TDP-43 models of neurodegeneration. *Geroscience* **44**, 747–761 (2022).
33. A. Calixto, D. Chelur, I. Topalidou, X. Chen, M. Chalfie, Enhanced neuronal RNAi in C. elegans using SID-1. *Nat. Methods* **7**, 554–559 (2010).
34. L. Galganski, M. O. Urbanek, W. J. Krzyzosiak, Nuclear speckles: Molecular organization, biological function and role in disease. *Nucleic Acids Res.* **45**, 10350–10368 (2017).
35. M. MacMorris *et al.*, A novel family of C. elegans snRNPs contains proteins associated with trans-splicing. *RNA* **13**, 511–520 (2007).
36. E. Lester *et al.*, Tau aggregates are RNA-protein assemblies that mislocalize multiple nuclear speckle components. *Neuron* **109**, 1675–1691.e1679 (2021).
37. H. Tanaka *et al.*, The intellectual disability gene PQBP1 rescues Alzheimer's disease pathology. *Mol. Psychiatry* **23**, 2090–2110 (2018).
38. P. J. McMillan *et al.*, Pathological tau drives ectopic nuclear speckle scaffold protein SRRM2 accumulation in neuron cytoplasm in Alzheimer's disease. *Acta. Neuropathol. Commun.* **9**, 117 (2021).
39. İ Ilik *et al.*, SON and SRRM2 are essential for nuclear speckle formation. *Elife* **9**, e60579 (2020).
40. S. Alberti, D. Dormann, Liquid-liquid phase separation in disease. *Annu. Rev. Genet.* **53**, 171–194 (2019).
41. S. Brenner, The genetics of Caenorhabditis elegans. *Genetics* **77**, 71–94 (1974).
42. E. A. De Stasio, S. Dorman, Optimization of ENU mutagenesis of Caenorhabditis elegans. *Mutat. Res.* **495**, 81–88 (2001).
43. A. Paix, A. Folkmann, D. Rasoloson, G. Seydoux, High efficiency, homology-directed genome editing in Caenorhabditis elegans using CRISPR-Cas9 ribonucleoprotein complexes. *Genetics* **201**, 47–54 (2015).
44. G. A. Dokshin, K. S. Ghanta, K. M. Piscopo, C. C. Mello, Robust genome editing with short single-stranded and long, partially single-stranded dna donors in. *Genetics* **210**, 781–787 (2018).
45. J. Schindelin *et al.*, Fiji: An open-source platform for biological-image analysis. *Nat. Methods* **9**, 676–682 (2012).
46. P. Lamesch *et al.*, C. elegans ORFeome version 3.1: Increasing the coverage of ORFeome resources with improved gene predictions. *Genome Res.* **14**, 2064–2069 (2004).